

340 A Combining the Additive and Functional Threat Models

341 Here we provide a proof of Theorem [1](#).

342 **Threat model** Let \mathbf{x} be a grayscale image with $n \geq 2$ pixels, i.e. $\mathbf{x} \in [0, 1]^n = \mathcal{X}^n$. Let t_{add} be
 343 an additive threat model where the ℓ_∞ distance between input and adversarial example is bounded
 344 by ϵ_1 , i.e. $\|(\delta_1, \dots, \delta_n)\|_\infty \leq \epsilon_1$. Let t_{func} be a functional threat model where $f(x) = cx$ for some
 345 $c \in [1 - \epsilon_2, 1 + \epsilon_2]$ and let $\epsilon_2 > \epsilon_1 > 0$. The additive threat model allows individually changing each
 346 pixel’s value by up to ϵ_1 ; the functional threat model allows darkening or lightening the entire image
 347 by up to a proportion of ϵ_2 . Both of these are arguably imperceptible perturbations for small enough
 348 ϵ_1 and ϵ_2 . We also consider $t_{\text{combined}} = t_{\text{add}} \circ t_{\text{func}}$:

$$t_{\text{combined}}(\mathcal{S}) \triangleq \left\{ (cx_1 + \delta_1, \dots, cx_n + \delta_n) \left| \begin{array}{l} (x_1, \dots, x_n) \in \mathcal{S} \\ |\delta_i| \leq \epsilon_1 \\ c \in [1 - \epsilon_2, 1 + \epsilon_2] \end{array} \right. \right\} \quad (3)$$

349 This combined threat model allows darkening or lightening the image, followed by changing each
 350 pixel value individually by a small amount.

351 **Theorem 1** (restated). Let $\mathcal{S} \in \mathcal{P}(\mathcal{X}^n)$ be a set of inputs such that \mathcal{S} contains an image that is not
 352 too dark; that is, $\exists \mathbf{x} \in \mathcal{S}$ for which $\exists x_i$ s.t. $x_i > \epsilon_1/\epsilon_2$. Then

$$t_{\text{combined}}(\mathcal{S}) \supsetneq t_{\text{add}}(\mathcal{S}) \cup t_{\text{func}}(\mathcal{S}) \quad \text{or equivalently} \quad \exists \tilde{\mathbf{x}} \text{ s.t. } \begin{array}{l} \tilde{\mathbf{x}} \in t_{\text{combined}}(\mathcal{S}) \\ \tilde{\mathbf{x}} \notin t_{\text{add}}(\mathcal{S}) \cup t_{\text{func}}(\mathcal{S}) \end{array}$$

353 *Proof.* The above two statements are equivalent, so we focus on the formulation on the right. We
 354 calculate $\tilde{\mathbf{x}}$ and show that it satisfies the given criteria. Let $\mathbf{x} \in \mathcal{S}$ such that $\exists x_i$ s.t. $x_i > \epsilon_1/\epsilon_2$.
 355 Without loss of generality, assume that in particular $x_2 > \epsilon_1/\epsilon_2$. Then let

$$\tilde{\mathbf{x}} = ((1 - \epsilon_2)x_1 + \epsilon_1, (1 - \epsilon_2)x_2, \dots, (1 - \epsilon_2)x_n)$$

356 First, we show that $\tilde{\mathbf{x}} \in t_{\text{combined}}(\mathcal{S})$. Using the definition of t_{combined} in [\(3\)](#), we set $c = 1 - \epsilon_2$,
 357 $\delta_1 = \epsilon_1$, and $\delta_2 = \dots = \delta_n = 0$, which generates $\tilde{\mathbf{x}}$. These values clearly satisfy the constraints in
 358 [\(3\)](#).

359 Second, we prove that $\tilde{\mathbf{x}} \notin t_{\text{add}}(\mathcal{S})$ by contradiction. Say that $\tilde{\mathbf{x}} \in t_{\text{add}}(\mathcal{S})$. Then $\exists \delta_1, \delta_2, \dots, \delta_n$
 360 such that $\tilde{x}_i = x_i + \delta_i$ and $\|\delta_i\| \leq \epsilon_1$. Consider δ_2 , which must satisfy $\tilde{x}_2 = (1 - \epsilon_2)x_2 = x_2 + \delta_2$,
 361 or alternatively $\delta_2 = x_2 - (1 - \epsilon_2)x_2 = \epsilon_2 x_2$. However, $x_2 > \epsilon_1/\epsilon_2$ implies that $\delta_2 > \epsilon_1$, which is
 362 a contradiction since the constraints on t_{add} specify that $|\delta_2| \leq \epsilon_1$. Thus, $\tilde{\mathbf{x}} \notin t_{\text{add}}(\mathcal{S})$.

363 Third, we prove that $\tilde{\mathbf{x}} \notin t_{\text{func}}(\mathcal{S})$, again by contradiction. Say that $\tilde{\mathbf{x}} \in t_{\text{func}}(\mathcal{S})$. Then $\exists c \in$
 364 $[1 - \epsilon_2, 1 + \epsilon_2]$ such that $\tilde{x}_i = cx_i$ for all i . Considering $i = 1, 2$, we have the following system of
 365 equations:

$$\begin{aligned} \tilde{x}_1 &= cx_1 = (1 - \epsilon_2)x_1 + \epsilon_1 \\ \tilde{x}_2 &= cx_2 = (1 - \epsilon_2)x_2 \end{aligned}$$

366 From the second equation, we have $c = 1 - \epsilon_2$. However, using this in the first equation gives
 367 $(1 - \epsilon_2)x_1 = (1 - \epsilon_2)x_1 + \epsilon_1$, which implies $0 = \epsilon_1$. This is a contradiction since $\epsilon_1 > 0$, showing
 368 that $\tilde{\mathbf{x}} \notin t_{\text{func}}(\mathcal{S})$. ■

369 B Experimental Setup

370 We implement ReColorAdv using the `mister_ed` library [\[9\]](#) and PyTorch [\[16\]](#). Adversarial examples
 371 are generated by 100 iterations of PGD using the Adam optimizer [\[10\]](#) with learning rate 0.001.
 372 After all iterations have completed, we choose the result of the iteration with the lowest loss as the
 373 adversarial example.

374 When combining attacks, we apply multiple attacks sequentially to the input example and optimize
375 over the parameters of all attacks simultaneously, similarly to Jordan et al. [9].

376 In all adversarial training experiments on CIFAR-10, we begin with a trained ResNet32 [8] and then
377 train it further on batches which are half original training data and half adversarial examples. We
378 adversarially train with a batch size of 500 for 50 epochs. We preprocess images after adversarial
379 perturbation, but before classification, by standardizing them based on the mean and standard
380 deviation of each channel for all images in the dataset. The CIFAR-10 dataset can be obtained from
381 <https://www.cs.toronto.edu/~kriz/cifar.html>.

382 In CIELUV color space (see section 4.1), we define

$$(c_1, c_2, c_3) = \left(\frac{L}{100}, \frac{U + 100}{200}, \frac{V + 100}{200} \right) \quad (4)$$

383 so that $(c_1, c_2, c_3) \in [0, 1]^3$.

384 For the experiments described in section 5.3, we use LPIPS v0.1 with AlexNet.

385 B.1 Regularization Parameters

386 The objective function and constraints described in section 4 include a number of constants that can
387 be used to regularize the outputs of the ReColorAdv attack. Changing these constants alters the
388 strength of the attack and the perceptual similarity of a generated adversarial example to the input.

389 First, ϵ_1 , ϵ_2 , and ϵ_3 control the maximum amount by which a color in \mathbf{x} can be changed to produce
390 $\tilde{\mathbf{x}}$. For RGB color space, we set $\epsilon_1 = \epsilon_2 = \epsilon_3 = 0.1$; that is, each channel of a color can change by
391 up to $\sim 25/255$. This is greater than the usual $\epsilon = 8/255$ allowed for adversarial examples, but we
392 find that the uniform perturbation used by the functional threat model allows each pixel to change
393 by a greater amount while remaining almost indistinguishable. For the CIELUV color space, we let
394 $\epsilon_1 = \epsilon_2 = \epsilon_3 = 0.06$. This corresponds to a maximum change of 6 in L and a maximum change of 3
395 in U and V , since we find that changes in luma are usually less noticeable than changes in chroma.
396 The ϵ_i values for RGB and CIELUV color spaces result in similar total amounts of perturbation, but
397 the CIELUV color space allows the perturbation to be greater in areas where it is less noticeable.

398 Second, we can control the resolution of the grid \mathcal{G} over which the perturbation function $f(\cdot)$ is
399 parameterized. Let $R_1 \times R_2 \times R_3$ be the resolution of \mathcal{G} . Lowering the resolution in a particular
400 dimension acts as a regularizer because it allows less variation in how colors are transformed along
401 that dimension. For RGB color space, we use $R_1 = R_2 = R_3 = 25$. However, for CIELUV color
402 space, we use $R_1 = 16$ and $R_2 = R_3 = 32$. With a high R_1 value, we find that the attack sometimes
403 recolors different values of a particular hue very differently. For instance, the attack might make the
404 light parts of a white car green and the dark parts purple. Lowering R_1 forces the attack to alter these
405 colors more similarly.

406 Finally, λ controls the importance of the smoothness optimization term $\mathcal{L}_{\text{smooth}}$. We always set
407 $\lambda = 0.05$.

408 C Learning Rate Experiments

409 We consistently use Adam with a learning rate of 0.001 throughout the main paper to craft adversarial
410 examples. However, we also experimented with a learning rate of 0.01. The results of these
411 experiments are shown below, similar to table 1. All numbers reported are accuracy over the CIFAR-
412 10 test set. Each column corresponds to an attack and each row corresponds to a model trained against
413 a particular attack. C(-RGB) is ReColorAdv using CIELUV (RGB) color space, D is delta attack,
414 and S is StAdv attack. TRADES is the method of Zhang et al. [26]. For classifiers marked (B&W),
415 the images are converted to black-and-white before classification. The learning rate used in an attack
416 is marked above that attack or to the right when the attack is used in adversarial training. There are a
417 couple interesting conclusions that can be drawn from this experiment:

- 418 • The higher learning rate (0.01) is stronger against TRADES and undefended networks. A
419 ReColorAdv + StAdv + delta (C+S+D) attack with learning rate 0.01 against a TRADES-
420 trained classifier reduces its accuracy to just 6.0%, compared with 10.1% at learning rate
421 0.001.

422
423
424
425
426
427

- Adversarial training against an attack at the higher learning rate (0.01) increases robustness against that attack but lowers it against other attacks. For instance, consider the network defended against C+S+D with learning rate 0.01. This network achieves 15.0% accuracy against attacks of the same type, but the accuracy decreases to 7.1% against some other attacks. In contrast, adversarial training against attacks at the lower learning rate (0.001) leads to more robustness across different attacks.

428

Defense	LR	Attack (learning rate = 0.01)								
		None	C-RGB	C	D	S	C+S	C+D	S+D	C+S+D
Undefended		92.3	5.1	3.8	0.0	1.5	1.5	0.0	0.0	0.0
C	0.01	87.8	37.4	45.5	4.7	3.2	2.9	1.2	0.2	0.4
D	0.01	88.8	40.4	22.7	32.7	4.2	4.3	15.0	5.0	4.0
S	0.01	89.3	11.5	9.8	0.3	29.0	9.5	0.4	0.4	0.3
C+S	0.01	90.5	27.0	24.3	2.8	31.4	23.0	2.1	2.8	2.1
C+D	0.01	88.3	46.3	32.7	34.4	6.0	5.4	22.6	4.7	4.8
S+D	0.01	88.0	25.3	17.4	28.4	9.3	8.1	22.6	17.0	13.9
C+S+D	0.01	89.0	32.3	23.8	29.8	13.4	11.4	26.1	17.4	15.0
C	0.001	89.2	37.2	46.6	5.1	3.4	3.0	1.1	0.3	0.3
D	0.001	84.7	72.9	57.4	30.8	12.2	11.2	12.6	2.4	1.8
S	0.001	82.7	14.9	11.9	0.5	22.2	6.7	0.1	0.2	0.1
C+S	0.001	82.3	37.5	40.4	5.9	18.5	13.1	1.9	0.9	0.8
C+D	0.001	84.3	70.8	60.0	33.8	9.4	8.7	18.1	1.8	1.9
S+D	0.001	82.0	65.2	49.9	35.0	18.5	14.0	16.5	5.5	4.5
C+S+D	0.001	82.3	65.8	53.0	34.8	16.8	14.7	18.3	5.1	5.0
TRADES		84.2	79.7	69.2	53.5	21.0	17.8	33.8	6.6	6.0
Undefended (B&W)		87.9	4.7	4.8	0.0	1.6	1.5	0.0	0.1	0.0
C (B&W)	0.01	84.7	40.4	41.7	4.5	2.4	2.4	1.0	0.2	0.3
C (B&W)	0.001	85.6	37.8	40.7	4.0	2.5	2.5	0.7	0.3	0.3

Defense	LR	Attack (learning rate = 0.001)								
		None	C-RGB	C	D	S	C+S	C+D	S+D	C+S+D
Undefended		92.3	8.3	5.3	0.0	2.2	1.8	0.0	0.0	0.0
C	0.01	87.8	46.2	48.4	5.9	4.5	4.4	1.6	0.3	0.7
D	0.01	88.8	43.7	25.4	26.4	4.1	3.8	15.7	8.3	7.9
S	0.01	89.3	18.7	13.9	0.4	13.8	8.4	0.8	0.6	0.9
C+S	0.01	90.5	39.1	32.3	4.3	22.7	17.5	2.8	3.5	3.3
C+D	0.01	88.3	49.1	35.6	29.2	5.3	5.4	20.3	8.7	8.3
S+D	0.01	88.0	25.8	17.7	10.7	4.5	4.1	9.3	6.1	5.9
C+S+D	0.01	89.0	33.9	24.9	15.7	7.5	7.1	13.0	8.4	8.5
C	0.001	89.2	47.4	50.3	5.9	4.6	4.6	1.7	0.5	0.9
D	0.001	84.7	77.3	61.9	32.8	18.6	17.2	17.3	4.3	4.2
S	0.001	82.7	20.3	15.7	0.8	29.9	10.7	0.2	0.2	0.2
C+S	0.001	82.3	47.2	44.6	7.5	26.2	20.2	3.5	2.2	2.0
C+D	0.001	84.3	74.7	63.5	35.2	14.0	13.4	22.2	4.5	4.2
S+D	0.001	82.0	69.3	53.9	36.5	26.4	21.1	21.7	9.6	8.0
C+S+D	0.001	82.3	70.1	56.4	35.5	25.5	21.4	23.4	10.0	8.5
TRADES		84.2	81.6	72.8	53.7	31.2	27.5	39.3	11.1	10.1
Undefended (B&W)		87.9	7.3	6.1	0.0	1.6	1.6	0.0	0.0	0.0
C (B&W)	0.01	84.7	49.3	44.9	5.4	4.1	3.8	1.6	0.5	0.7
C (B&W)	0.001	85.6	46.7	43.8	5.0	3.5	3.8	1.3	0.4	0.7

429

430 **D Non-Additive Threat Models**

431 Here, we discuss some other non-additive adversarial threat models that have been explored in the
432 literature and how our work differs from them.

433 **Spatial Threat Models** Some recent work has focused on *spatial threat models*, which allow for
434 slight perturbations of the locations of features in an input rather than perturbations of the features
435 themselves. Xiao et al. [23] propose StAdv, which optimizes the parameters of a smooth flow field
436 that moves each pixel of an input image by a small, bounded distance to generate an example that
437 fools the classifier. Wong et al. [22] bound the Wasserstein distance between the original input and
438 the adversarial example. Engstrom et al. [3] apply a small rotation and translation to an input image
439 to generate a misclassification.

440 **Other Threat Models** A few papers have focused on threat models that are neither additive or
441 spatial. Zeng et al. [25] perturb the properties of a 3D renderer to render an image of an object which
442 is unrecognizable to a classifier or other machine learning algorithm. Hosseini and Poovendran [6]
443 propose "Semantic Adversarial Examples," which allow modifications of the input image's hue and
444 saturation. Hosseini et al. [7] also explore inverting images to cause misclassification. These latter
445 two papers can be considered as special examples of functional threat models. In the first, each
446 pixel's hue and saturation is shifted by the same amount; that is, each pixel is transformed by the
447 function $f(h, s, v) = (h + \delta_h, s + \delta_s, v)$. In the second, each pixel is inverted, i.e. each pixel channel
448 is transformed by the function $f(x_i) = 1 - x_i$. However, the authors do not propose a general
449 framework for these types of attacks, as we do. Furthermore, the adversarial examples generated
450 by these attacks are often not realistic and not imperceptible. For example, their crafted adversarial
451 examples include green skies, purple fields of grass, and inverted street signs—unlike our proposed
452 ReColorAdv attack, which results in imperceptible changes.

453 **E Additional Images**



Figure 7: More adversarial examples like those in figure 2, generated by ReColorAdv against an Inception-v4 classifier on ImageNet. Top row: original images; middle row: adversarial examples; bottom row: magnified difference.

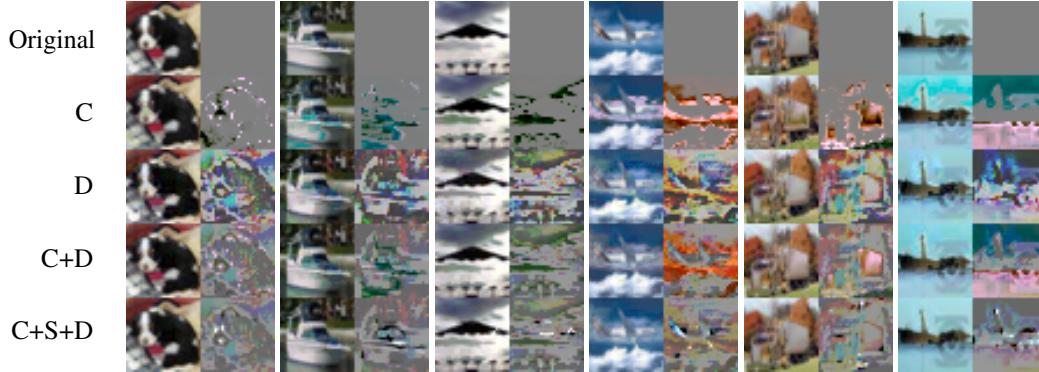


Figure 8: More adversarial examples like those in figure 5 generated with combinations of attacks against a CIFAR-10 WideResNet trained using TRADES. C is ReColorAdv, D is delta attack, and S is StAdv attack [23]. The difference from the original is shown to the right of each example. Combinations of attacks tend to produce less perceptible changes than the attacks do separately.

454 F Lipschitz Regularization

455 In addition to the regularizations defined in section 3.1, we can also enforce that the perturbation
 456 function $f(\cdot)$ in a functional threat model is Lipschitz for some suitably small κ :

$$\mathcal{F}_{\text{lips}} \triangleq \{f : \mathcal{X} \rightarrow \mathcal{X} \mid \forall x_1, x_2 \in \mathcal{X} \|f(x_1) - f(x_2)\| \leq \kappa \|x_1 - x_2\|\} \quad (5)$$

457 $\mathcal{F}_{\text{lips}}$ requires some smoothness in the perturbation function $f(\cdot)$, ensuring that similar features in the
 458 input are mapped to similar features in the adversarial example. However, one disadvantage of $\mathcal{F}_{\text{lips}}$
 459 is that it includes constant functions $f(x) = c$, i.e. functions which map every feature to a single
 460 value, removing salient features from the input. Thus, we ultimately use $\mathcal{F}_{\text{smooth}}$ instead.